

Emerging attractors and the transition from dissipative to conservative dynamics

Christian S. Rodrigues*, Alessandro P. S. de Moura, and Celso Grebogi

Department of Physics, King's College, University of Aberdeen - Aberdeen AB24 3UE, UK.

(Dated: August 28, 2008)

The topological structure of basin boundaries plays a fundamental role in the sensitivity to the initial conditions in chaotic dynamical systems. Herewith we present a study on the dynamics of dissipative systems close to the Hamiltonian limit, emphasising the increasing number of periodic attractors and on the structural changes in their basin boundaries as the dissipation approaches zero. We show numerically that a power law with nontrivial exponent describes the growth of the total number of periodic attractors as the damping is decreased. We also establish that for small scales the dynamics is governed by *effective* dynamical invariants, whose measure depends not only on the region of the phase space, but also on the scale under consideration. Therefore, our results show that the concept of effective invariants is also relevant for dissipative systems.

PACS numbers: 05.45.Ac 61.43.Hv

Keywords: effective fractal dimension, limit conservative - dissipative, topological structure, fractal basin boundary

I. INTRODUCTION

Many dynamical processes have been shown to possess coexisting metastable states, and their dynamics can be highly sensitive to the initial conditions. Some examples include neural behaviour [1, 2], rain events [3], earthquakes' dynamics [4, 5], molecular dynamics [6], among others. Their correct interpretation requires an understanding of dynamical systems with very low dissipation, lying in between the strongly dissipative limit and the conservative one. In spite of the importance of this problem, there are few systematic studies of the low-dissipation limit and the transition from dissipative to conservative dynamics. This is the problem we address in this paper.

In Hamiltonian systems, chaotic regions typically coexist with regions of regular motion around the stable periodic orbits, also known as Kolmogorov-Arnold-Moser (KAM) invariant tori. Chaotic trajectories have intermittent behaviour and spend long times sporadically near the border of regular islands. This stickiness to the KAM tori makes their dynamics fundamentally different from that of hyperbolic chaotic systems, since even small islands can exert great influence on the global dynamics [7, 8, 9]. On the other hand, strongly dissipative systems are characterised as having only one or few attractors to which all the initial conditions eventually converge. These two regimes could not be more different from each other; however, if the dissipation decreases to zero, the phase space structure of the dissipative systems must evolve in such a way as to approach the complex hierarchical organisation found in Hamiltonian systems. How this transformation occurs is far from obvious.

Despite the existence of extensive investigations on strongly dissipative and on Hamiltonian systems, very

little is known about properties of systems close to the border between dissipative and conservative dynamics, where many coexisting periodic attractors are present [10]. In this paper we investigate the growth of the number of periodic attractors and how the topology of the phase space evolves when the dissipation is reduced. We obtain numerically a power law describing the growth of the number of periodic attractors as the damping goes to zero. When the system is close to the Hamiltonian limit, we find that high-period periodic attractors become increasingly important in the system's dynamics, in contrast to the case with high dissipation. These *emerging attractors* proliferate ever more rapidly as the dissipation decreases. Moreover, we argue that although this number can be extremely high for small dissipation, we expect it to be finite (for non-zero dissipation), as conjectured recently [11, 12]. The power law or the number of attractors with dissipation, found in this work, corroborates this conjecture. Another important finding in this paper is that for low levels of damping the dynamics is characterised by *effective invariants*, a concept previously used in the context of non-hyperbolic dynamics of Hamiltonian systems [7]. We study specifically the *effective fractal dimension*, which we show to depend on the scale and also on the region of the phase space. Therefore we show that effective dynamics is relevant also for dissipative systems, and not only for Hamiltonian ones.

This paper is organised as follows. We introduce the dynamical system which was utilised in our analysis and revisit in this context the problem of the number of co-existent attractors in Sec. II. It is followed, Sec. III, by a discussion regarding the topology of the phase space in the low-dissipation limit. In Sec. IV we introduce effective invariants and define the effective fractal dimension for weakly dissipative systems. Finally, Sec. V brings our conclusions.

*Electronic Address: c.rodrigues@abdn.ac.uk

II. NUMBER OF PERIODIC ATTRACTORS

A paradigmatic system that allows the investigation of the transition from the dissipative to the conservative limit is the *single rotor map*, obtained from the mechanical pendulum kicked periodically at times nT , $n \in \mathbb{N}^+$, with force f_0 [13]:

$$\begin{aligned} x_{n+1} &= x_n + y_n \pmod{2\pi} \\ y_{n+1} &= (1 - \nu)y_n + f_0 \sin(x_n + y_n), \end{aligned} \quad (1)$$

where $x \in [0, 2\pi]$ corresponds to the phase, $y \in \mathbb{R}$ to the angular velocity, and $\nu \in [0, 1]$ is the damping parameter. For $\nu = 0$, the well known area preserving standard map analysed by Chirikov [14] is recovered. For $\nu = 1$, we recover the circle map with zero rotation number.

Previous work has considered the question of the number of attractors for this system [10]. They have derived an analytical expression for the number of period-1 primary attractors:

$$N_{p1} = 2I\left(\frac{f_0}{2\pi\nu}\right) + 1, \quad (2)$$

where $I(\cdot)$ denotes the integer part of the expression in brackets. However, this expression is only valid in a limited parameter interval, and does not hold in the low-dissipative limit. As pointed out in Ref. [10], numerical detection of attractors with high period is a difficult task. The reason is the extremely small size of their basins of attraction, what requires computation using very thin grids. Adding to this, they have short lifetime in the space of parameters. Therefore it is necessary to follow a great number of initial conditions in order to be able to detect them.

Here we overcome this problem. Instead of choosing an *a priori* fixed number of initial conditions in a preset grid, as previously done in Ref. [10] and elsewhere, we fix the nonlinearity $f_0 = 4.0$ for a given damping ν and then iterate an ensemble of randomly chosen initial conditions with uniform distribution on a bounded region of the phase space. Therefore, the chance for an attractor to be found does not depend on our particular choice for the grid. For the dissipative case the dynamics takes place in the cylinder $\Gamma = [0, 2\pi] \times \mathbb{R}$ and the area where the initial conditions are chosen depends on the damping. Since $\nu > 0$, from the second equation in the map (1), one gets $|y_{k+1}| \leq (1 - \nu)|y_k| + f_0$, so if $|y_k| > f_0/\nu \Rightarrow |y_{k+1}| < |y_k|$. Hence the attractors are found in $\Lambda \subset \Gamma$, with $\Lambda = [0, 2\pi] \times [-y_{max}, y_{max}]$, where $y_{max} = f_0/\nu$.

In order to detect attractors, even with very small basins of attraction, we keep iterating new, randomly chosen initial conditions $(x_0, y_0) \in \Lambda$ until their trajectories converge to some periodic attractor. We used up to 2×10^5 iterations; no matter the damping, this provides a convergence of more than 99.5% of the initial conditions. We have ignored the remaining trajectories (which may include chaotic orbits), regarding them as not being statistically representative. It is known that for this and

similar systems, almost all attractors consist of periodic orbits. We keep iterating new initial conditions until we fail to find new attractors. This was determined by the criterion that whenever the total number of detected attractors did not change for the last 10^6 initial conditions, we assume that all the detectable attractors have been found. This is illustrated in Fig. 1 for $\nu = 0.0035$. We repeat this procedure for different values of ν , in order to find how the total number of periodic attractors changes with damping. Notice that the area of the phase space where the trajectories are trapped grows as we decrease

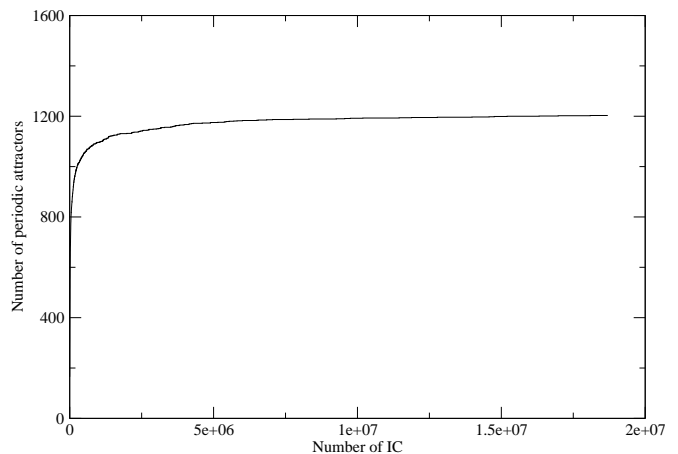


FIG. 1: Total number of periodic attractors detected for a specific value of the dissipation ν , as a function of the number of initial conditions randomly chosen in Λ and evolved according to the map. The used parameters for the map (1) were $f_0 = 4.0$, and $\nu = 0.0035$.

The question regarding the finiteness of the number of attractors and their denseness on the phase space has been considered before and it is widely regarded as one of the most important open problems still to be answered in Dynamical Systems Theory [11]. Among many conjectures, it has been initially proposed that the number of attractors was infinite [15]. Afterwards it has been proved that this should only hold for a zero measure set of parameter values, though dense in some interval [16]. Recently it has also been conjectured by Palis that the total number of attractors should be finite [12].

To investigate this issue using our system (1) as a testing ground, we calculate the number of attractors as described above, and see how this depends on the dissipation ν as it is decreased and approaches the conservative limit, i.e. $\nu \rightarrow \varepsilon > 0$. Figure 2 shows a *log-log* plot of our data, yielding a power law describing the dependence of the total number of periodic attractors on ν . Numerical fitting gives us the following law:

$$N_{TP} \approx 1.26 \cdot \nu^{-1.21}, \quad (3)$$

where N_{TP} is the total number of detected periodic attractors. Although we cannot claim the above result is

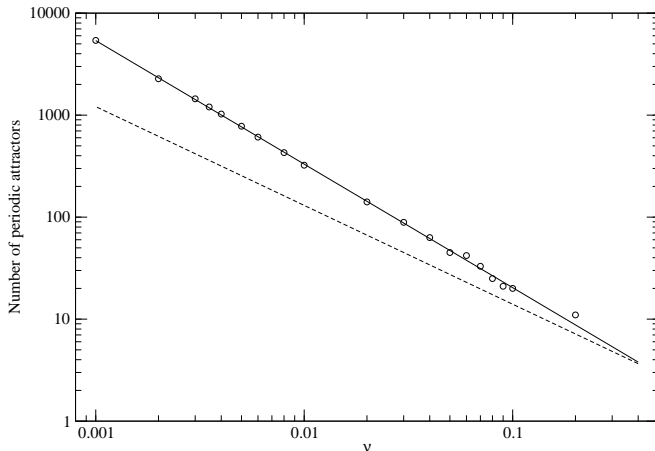


FIG. 2: Total number of periodic attractors which were detected numerically (circles) for different values of ν , and fixed $f_0 = 4.0$. The fitting of the power law (solid line) is also shown; compare to the number of period 1 attractors expected from Eq. (2) (dashed line). The divergence from one curve to the other is clear, showing the important contribution of high period attractors in the regime of small damping.

a mathematical proof, our results seem to uphold Palis' conjectures [11, 12], i.e., for any arbitrarily small $\varepsilon > 0$, the limit of Eq. (3), as $\lim_{\nu \rightarrow \varepsilon^+} N_{TP}$ predicts a finite number of attractors for the system, though this number can be very high for small ε .

Now we want to compare our power law for the growth of the total number of periodic attractors with the formula (2) [10] for the number of period 1 attractors. We observe in Fig. 2 that when the damping is decreased the contribution of higher period periodic attractors becomes important for the total number of detected attractors. The main reason is that the *lifetime* of a stable, periodic orbit in parameter space increases as damping is reduced. By *lifetime* of an orbit we mean the range in parameter space for which the orbit exists, without undergoing any bifurcation. Since the higher the period of an attractor, the smaller its lifetime interval in parameter space [10], the extension of lifetime for small damping promotes the overlap of different periodic orbits in the space of parameters, which was not possible before. Equation (2) is only valid within the parameter intervals where none of the period 1 attractors has undergone period doubling [10]. Since some of the period

1 attractors may have gone through such process for the parameters in Fig. 2, the difference between the expected number of period 1 attractors and the total number of attractors can be even larger than that inferred from the above argument.

Although some attractors may have their basins of attraction so tiny that even by iterating a huge number of initial conditions is not enough to numerically detect them, Fig. 1 shows that the number of attractors which was detected is asymptotic to a constant. Therefore, our result indicates that the number of attractors increases as a power law as the dissipation decreases, being finite for any given $\nu > 0$, though arbitrarily large for ν approaching zero. Even though the specific value of the exponent in Eq. (3) may be only valid for the map (1), the growth of the number of periodic attractors is a very generic property of weakly dissipative systems [17] which should not depend on the details of the system, since in the low-dissipative limit the system's phase-space approaches that of Hamiltonian systems, which have universal properties for all conservative systems. We therefore expect that the same behaviour reported here holds for other systems.

The natural question which arises now is the following: what happens to the topology of the phase space as new attractors continually appear with decreasing damping?

III. TOPOLOGY OF THE PHASE SPACE

We start this section with a qualitative picture of the transformations in phase space structure when the damping is decreased. Although one cannot draw definitive conclusions from this qualitative analysis, it motivates us to some further quantitative investigation, which will be tackled at the end of this section and in the next one. In order to obtain some clue about which topological changes occur when the damping is decreased, we begin by looking at the phase space for the system with constant forcing and high damping; In this case the system has only few periodic attractors. We then decrease ν , find the periodic attractors for the new parameter and plot their basins of attraction. Since we are now only interested in the general picture, the number of initial conditions is fixed at 2×10^6 .

If we follow the distributions of filaments of the largest basin of attraction in the phase space, we notice that their structure becomes more heterogeneous for different regions when the damping is decreased. This is illustrated in Fig. 3, where each colour (colour online) represents a set of initial conditions which converge to one of the attractors, i.e., different colours represent different

basins of attraction. In Fig. 3 (a), for which $\nu = 0.32$, we notice that the largest basin of attraction (in black) is spread all over the phase space in an intricate structure. Moreover, if we compare distinct regions of the phase space, there is a qualitative difference in the "density" of filaments of the largest basin of attraction. In particular, the farther the region is from the main at-

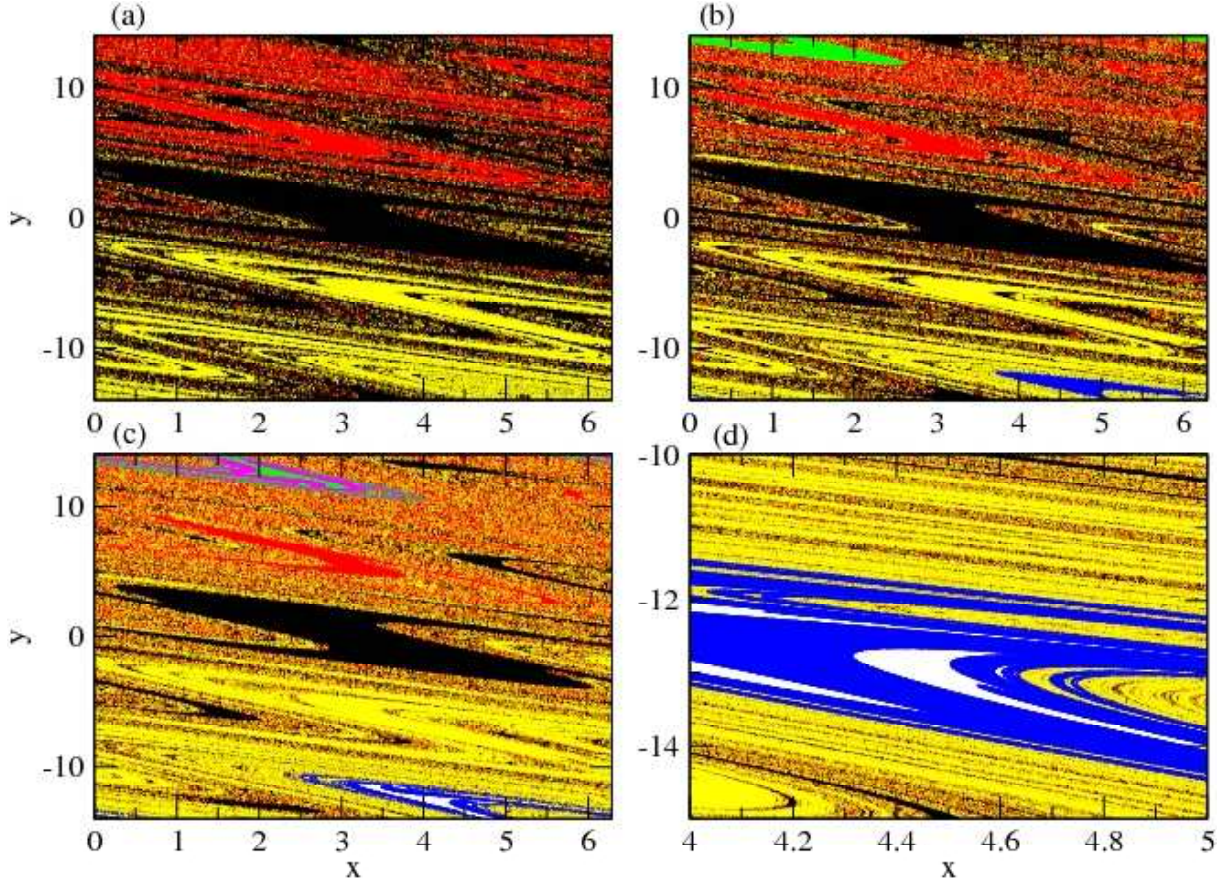


FIG. 3: (Colour online) Basins of attraction for $f_0 = 4.0$ and different values of ν . Each colour represents a set of initial conditions which converge to one of the attractors. In (a) $\nu = 0.32$, in (b) $\nu = 0.3$, in (c) $\nu = 0.2415$, and (d) is the blow up of a region $x \in [4, 5]$, $y \in [-15, -10]$ for $\nu = 0.2415$. We used 2×10^6 initial conditions for each one of the figures.

tractor, the thinner the filaments are. In Fig. 3 (b), for $\nu = 0.3$, we detect five attractors and the topology of the phase space, i.e., the spatial distribution of invariant sets, seems to become more complex. Going even further, for $\nu = 0.2415$ in Fig. 3 (c), we have seven attractors in the same region and the difference of density of those filaments is clearer. Figure 3 (d) is the blow up of the region $x \in [4, 5]$, $y \in [-15, -10]$ for $\nu = 0.2415$. The rescaling of the phase space shows the structure of the basins which seems to form a self similar pattern, as illustrated in Fig. 4.

As we decrease the damping even further, this process seems to carry on and the heterogeneity of the phase space keeps increasing. Furthermore, the difference of denseness of filaments for distinct regions of the phase space is seen by looking, for instance, at the largest basin of attraction for $\nu = 0.02$, and $f_0 = 4.0$. For these parameters we expect from Eq. (3) to find about 140 periodic attractors. The largest basin of attraction is responsible for about 36% of the initial conditions $(x_0, y_0) \in [0, 2\pi] \times [-\pi, \pi]$ [10]. This is illustrated in Fig. 5, which has been done by the iteration of an ensemble of 10^6 initial conditions.

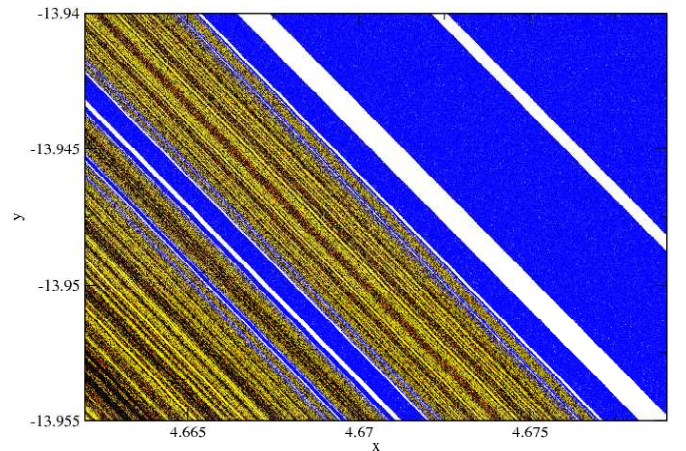


FIG. 4: (Colour online) Blow up of the region $x \in [4.662, 4.679]$, $y \in [-13.955, -13.94]$ for $\nu = 0.2415$ in Fig. 3 (d), showing the fractal cantor structure.

The structures we just presented are nothing but manifestations of the underlying invariant sets, i.e., the basin boundary is the stable manifold of an invariant set.

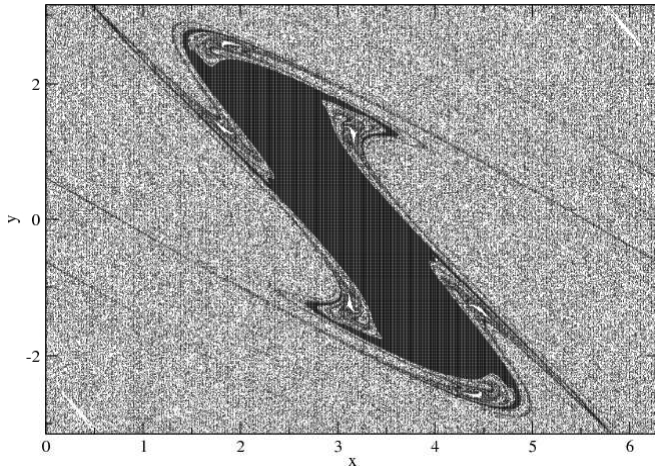


FIG. 5: The largest basin of attraction for $\nu = 0.02$ and $f_0 = 4.0$. The black points represent initial conditions which converge to the attractor formed from the main island. The initial conditions were chosen such that, $(x_0, y_0) \in [0, 2\pi] \times [-\pi, \pi]$. We used the same parameters as those used in Ref [10].

Therefore, if we define the boundary B in some region of the phase space embedded in the boundary as $S \cap B$, where S denotes some open set in phase space which contains part of the boundary B , we expect for a given ν the same fractal dimension of the basin boundary, i.e., $\dim(S \cap B)$ should be constant for different regions of the phase space, $\mathbf{R} \subset \Gamma$, as it has been conjectured in Ref. [18]. Nevertheless, for physically relevant scales, the heterogeneity in the distribution of the basins over the phase space, and hence the spatially heterogeneous distribution of invariant manifolds, suggests that coarse-grained measurements of quantities such as the fractal dimension should lead to different results depending on the region of the phase space and on the scale under consideration. The reason is that realistic measurements never take the limit of infinitely small scales, but must have a finite lower scale. Previous works in the context of Hamiltonian systems show that when the phase space has a heterogeneous structure such as in this case, one needs to go to exceedingly small scales to approach the mathematical value of the fractal dimension, which is unique and independent of the portion of the phase space used to calculate it. For physically realistic scales, an approximation to the fractal dimension (and similar quantities) is more appropriate to describe the system's dynamics; this approximation, called the *effective fractal dimension*, will depend on the position as well as on the considered scale. This will be presented in more detail in the next Section.

A finite-scale approximation of the fractal dimension of the basin boundary can be estimated using the uncertainty method [19]. This consists in iterating an ensemble of initial conditions (x_0, y_0) and check to which attractor they converge. Then we add a small perturbation ε to the initial conditions, say as $(x_0, y_0 + \varepsilon)$ and check

whether they change from one basin to another. We count the fraction of initial conditions that have changed their asymptotic state after being perturbed in this manner. This fraction, $f(\varepsilon)$ of ε -uncertain points, i.e., the fraction of initial conditions that change basins under an ε -size perturbation, scales as $f(\varepsilon) \sim \varepsilon^\alpha$, where α is related to the box counting dimension d of the basin boundary by $\alpha = D - d$, where D is the dimension of the phase space (For the map (1) we have $D = 2$).

In Fig. 6 we show the fraction of “uncertain” initial conditions as function of the size of perturbation ε [20].

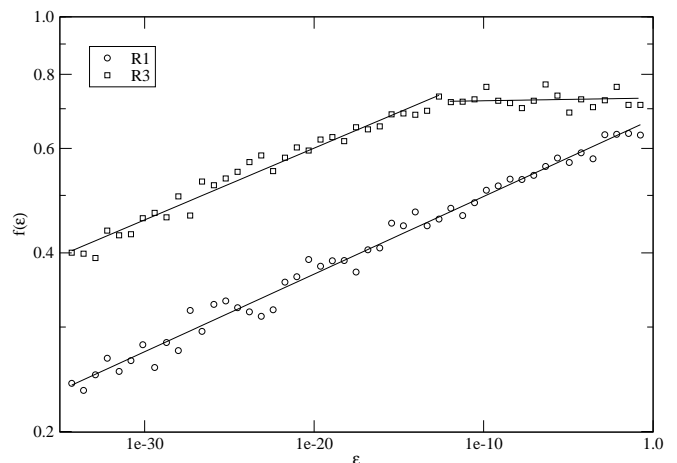


FIG. 6: Fraction of uncertain initial conditions $f(\varepsilon)$ as a function of the perturbation size ε for two different regions of the phase space. The utilised parameters were $f_0 = 4.0$, and $\nu = 0.08$.

The exponents $\alpha = \Delta \ln f(\varepsilon) / \Delta \ln \varepsilon$ can be computed over some decades. However, we notice in Fig. 6 that the slope assumes different values for distinct regions of the phase space. Moreover, it is clear that for $\varepsilon > 10^{-13}$, the estimated fractal dimension is larger for the region \mathbf{R}_3 , where the stable manifold is less dense. Only when we go down to $\varepsilon < 10^{-13}$ does the slope for the region \mathbf{R}_3 converges to the same value as of the region \mathbf{R}_1 , as expected: for small enough ε , the slope eventually converges to the true fractal dimension, which has a unique value [18]. We have computed $f(\varepsilon)$ for even smaller values of ν , and we have observed the same behaviour. However, for values as small as $\nu = 0.02$, even going down to $\varepsilon = 10^{-35}$ is sometimes not enough to obtain a convergence to a unique value of the estimated dimension in different regions. This shows that an effective dimension is indeed the relevant physical quantity to be considered also for weakly dissipative systems.

IV. EFFECTIVE FRACTAL DIMENSION

From the theoretical results regarding the fractal dimension of the basin boundary [18], we expect to have the

same fractal dimension for different regions of the phase space. However, the above discussion and results suggest that, for realistic scales, the behaviour for weakly dissipative systems can be quite different from the asymptotic one. Therefore it is sensible to describe the system in terms of *effective* invariants, a concept which has been used mostly in the context of non-hyperbolic Hamiltonian dynamical systems. [7]. As an example of effective invariants we use the definition of effective fractal dimension for a D -dimensional system, which depends on the region $\mathbf{R} \subset \Gamma$, and on the scale under consideration [22]. It is defined as

$$D_{eff}(R, \varepsilon) = D - \left. \frac{d \ln f(\varepsilon')}{d \ln \varepsilon'} \right|_{\varepsilon' = \varepsilon}, \quad (4)$$

where $f(\varepsilon')$ is the total uncertain phase space volume estimated as $\varepsilon'^D N(\varepsilon')$, and $N(\varepsilon')$ is the number of hypercubes of size ε' necessary to cover $S \cap B$.

We have computed the effective fractal dimension of the basin boundary for finite scales, for different values of ν , and for distinct regions in the phase space. The regions, $\mathbf{R}_i \subset \Gamma$, were chosen to be $\mathbf{R}_1 \equiv (x, y) \in [0, 1.5] \times [-1.0, -2.5]$, $\mathbf{R}_2 \equiv (x, y) \in [1.0, 2.5] \times [18.5, 20.0]$, and $\mathbf{R}_3 \equiv (x, y) \in [1.0, 2.5] \times [198.5, 200.0]$.

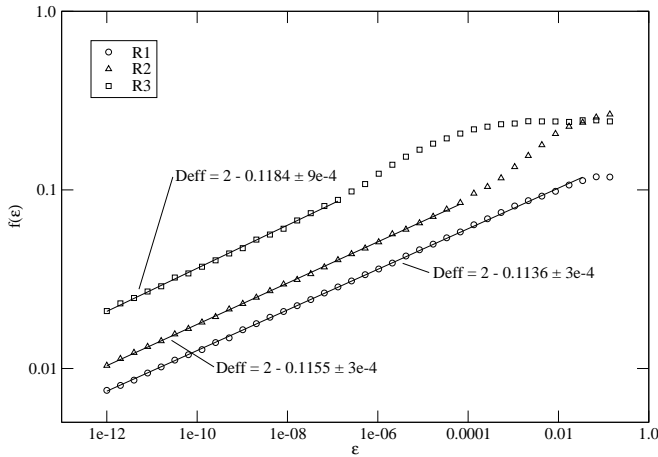


FIG. 7: Fraction of uncertain initial conditions $f(\varepsilon)$ scaling with the perturbation ε for three different regions of the phase space. The regions, $\mathbf{R}_i \subset \Gamma$, were defined as $\mathbf{R}_1 \equiv (x, y) \in [0, 1.5] \times [-1.0, -2.5]$, $\mathbf{R}_2 \equiv (x, y) \in [1.0, 2.5] \times [18.5, 20.0]$, and $\mathbf{R}_3 \equiv (x, y) \in [1.0, 2.5] \times [198.5, 200.0]$. The utilised parameters were $f_0 = 4.0$, and $\nu = 0.3$.

We have extracted the effective fractal dimension from Fig. 7 for $\nu = 0.3$ and $f_0 = 4.0$, where the system has apparently 5 periodic attractors. We notice that for \mathbf{R}_3 , where the stable manifold is less dense, starting from $\varepsilon = 10^{-1}$, the value of the effective fractal dimension is larger, but after few decades it converges to nearly the same as for \mathbf{R}_1 , i.e., $D_{eff} = 1.89$, where the stable manifold is denser. The same phenomenon is observed for \mathbf{R}_2 , though the convergence is faster than for \mathbf{R}_3 . When we decrease ν , hence increasing the number of attractors, even for $\varepsilon = 10^{-12}$, which is almost in the limit

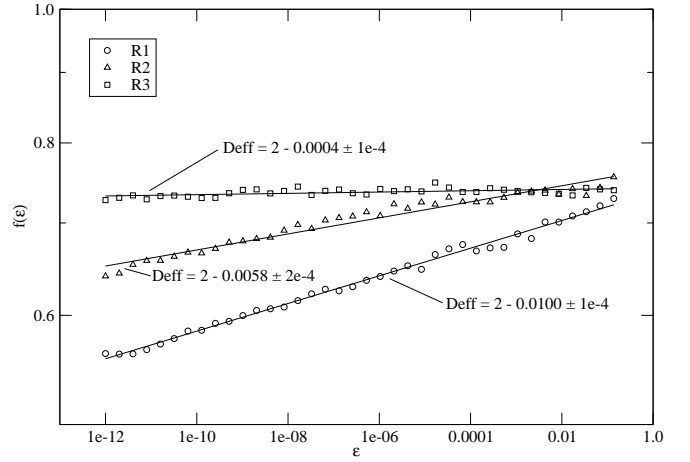


FIG. 8: Fraction of uncertain initial conditions $f(\varepsilon)$ scaling with the perturbation ε for three different regions of the phase space. The regions are the same as in Fig.7. The utilised parameters were $f_0 = 4.0$, and $\nu = 0.07$.

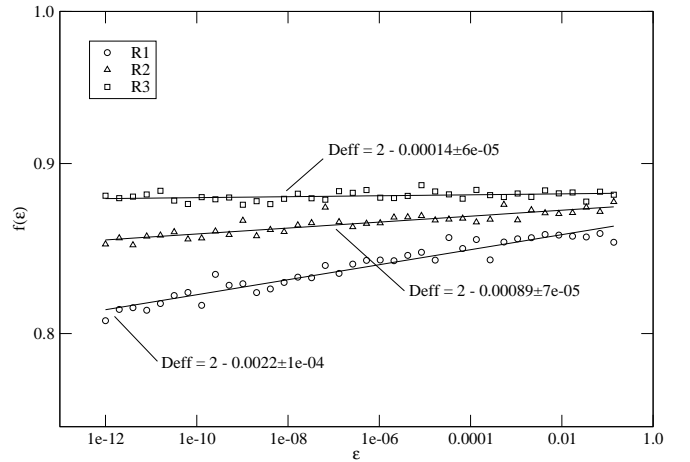


FIG. 9: Fraction of uncertain initial conditions $f(\varepsilon)$ scaling with the perturbation ε for three different regions of the phase space. The regions are the same as in Fig.7. The utilised parameters were $f_0 = 4.0$, and $\nu = 0.02$.

of normal computation and far beyond realistic measurement capacity, we do observe different values of effective fractal dimension for different regions, as it is shown in Fig. 8 and Fig. 9, for $\nu = 0.07$ and $\nu = 0.02$, respectively. We also notice that for a given region the exponent α becomes smaller as the damping is decreased. This indicates that for such weakly dissipative systems, the fractal dimension is very close to the dimension of the phase space. This is, of course, in accordance with the fact that for Hamiltonian systems ($\nu = 0$), the fractal dimension assumes its maximum value, i.e., D .

V. CONCLUSION

We have shown that the dynamics of weakly dissipative dynamical systems can be quite different from either the strongly dissipative systems or the Hamiltonian ones. When the damping is decreased, the number of periodic attractors increases. We have shown that the growth of the total number of attractors is described by a power law. In general, the interval in the space of parameters in which an attractor exists is smaller for high period periodic attractors. For small damping, attractors with different periods coexist in phase space, and the contribution of high period periodic attractors to the dynamics becomes important. Although the total number of attractors in the system is very high for low damping, our results strongly suggests that it remains finite for $\nu > 0$, supporting Palis' conjecture. The formation of new attractors as the damping decreases changes the topology of the phase space considerably. For low damping, the dynamics is better characterised by effective dynamical invariants, in a similar way to the case of non-hyperbolic Hamiltonian systems. These effective dynamical invari-

ant sets depend on the scale and they differ from one region to the other in the phase space. In particular, the effective fractal dimension of the basin boundary is larger for regions where the stable manifold is less dense. For a given region, the smaller the damping, the closer the effective fractal dimension is to the dimension of the phase space. Although we have used a specific example to illustrate our ideas, our results are generic since we have deal only with general characteristics of dynamical systems close to Hamiltonian case [12].

Acknowledgments

The authors thank E. G. Altmann for the careful reading of the manuscript and useful suggestions. C. S. R. thanks I. J. Rodrigues for illuminating discussion, and takes the opportunity to pay his tribute to J. S. Rodrigues (*in memoriam*), who gave him the firsts scientific hints. This work was supported by the School of Natural Sciences, University of Aberdeen.

-
- [1] N. Nagao, H. Nishimura, and N. Matsui, *Neural Processing Lett* **12**, 267 (2000).
 - [2] S. J. Schiff and K. Jerger and D. H. Duong and et al., *Nature* **370**, 615 (1994).
 - [3] O. Peters, and K. Christensen, *Phys. Rev. E* **66**, 036120 (2002).
 - [4] P. Bak, K. Christensen, L. Danon, and T. Scanlon, *Phys. Rev. Lett* **88**, 178501-1 (2002).
 - [5] M. Anghel, *Chaos Solit & Frac* **19**, 399 (2004).
 - [6] W. F. Wang, and P. P. Ong, *Phys. Rev. A* **55**, 1522 (1997).
 - [7] A. Motter, A. P. S. de Moura, C. Grebogi, and H. Kantz, *Phys. Rev. E* **65**, 026120 (2005).
 - [8] J. D. Meiss, J. R. Cary, J. D. Crawford, C. Grebogi, A. K. Kaufman, and H. D. I. Abarbanel, *Physica D* **6**, 375 (1983).
 - [9] E. G. Altmann, A. Motter, and H. Kantz, *Phys. Rev. E* **73**, 026207 (2006).
 - [10] U. Feudel, C. Grebogi, B. R. Hunt, and J. A. Yorke, *Phys. Rev. E* **54**, 71 (1996).
 - [11] J. Palis, *A global perspective for non-conservative dynamics*, Institute of Pure and Applied Mathematics (IMPA), preprint, 2005. See also references therein.
 - [12] J. Palis, *Astérisque* **261**, 335 (2000).
 - [13] G. M. Zaslavskii, *Phys. Lett. A* **69**, 145 (1978).
 - [14] B. Chirikov, *Phys. Rep. A* **52**, 265 (1979).
 - [15] S. E. Newhouse, *Topology* **13**, 9 (1974).
 - [16] L. Tedeschini-Lalli, and J. A. Yorke, *Commun. Math. Phys* **106**, 635 (1986).
 - [17] U. Feudel, and C. Grebogi, *Chaos* **7**, 597 (1997); *ibid*, *Phys. Rev. Lett.* **91**, 134102 (2003).
 - [18] C. Grebogi, H. E. Nusse, E. Ott, and J. A. Yorke, *in Lectures Notes in Mathematics* **1342**, 220 Ed by J. C. Alexander, Springer-Verlag, New York, 1988. See also references therein.
 - [19] C. Grebogi, S. W. McDonald, E. Ott, and J. A. Yorke, *Phys. Lett* **99A**, 415 (1983).
 - [20] The numerical simulations for $\varepsilon \leq 10^{-13}$ were carried out with high precision by using the MPFR C library for arbitrary precision [21], which seemed to be the best choice for trigonometric functions. However, the computational cost is relatively high in comparison to standard C precision. For the exponent uncertainty, we have iterated a sufficient number of initial conditions, in order to reach 400 uncertain points. Using standard precision, we have fixed this limit up to 10000.
 - [21] L. Fousse, G. Hanrot, V. Lefèvre, P. Pélissier, and P. Zimmermann, MPFR: A multiple-precision binary floating-point library with correct rounding. *ACM Trans. Math. Softw.* **33**, 13 (2007).
 - [22] Effective fractal dimension has been defined in a similar way for Hamiltonian system [7].